

Measurement of Curvature and Temperature using Multimode Interference Devices

J. R. Guzman-Sepulveda*¹, J. G. Aguilar-Soto², M. Torres-Cisneros¹, O. G. Ibarra-Manzano¹,
and D. A. May-Arrijo³

¹Nanobiophotonics Group, DICIS, Universidad de Guanajuato
Salamanca Guanajuato 36885, México

²Photonics and Optical Physics Laboratory, Optics Department, INAOE
Tonantzintla, Puebla 72000, México

³ Electronics Department, UAM Reynosa Rodhe, Universidad Autónoma de Tamaulipas
Reynosa, Tamaulipas 88779, México.

*Corresponding author: jrafael_guzmans@yahoo.com.mx

Abstract

In this paper we propose the fabrication, implementation, and testing of a novel fiber optic sensor based on Multimode Interference (MMI) effects for independent measurement of curvature and temperature. The development of fiber based MMI devices is relatively new and since they exhibit a band-pass filter response they can be used in different applications. The operating mechanism of our sensor is based on the self-imaging phenomena that occur in multimode fibers (MMF), which is related to the interference of the propagating modes and their accumulated phase. We demonstrate that the peak wavelength shifts with temperature variations as a result of changes in the accumulated phase through thermo-optics effects, while the intensity of the peak wavelength is reduced as the curvature increases since we start to lose higher order modes. In this way both measurements are obtained independently with a single fiber device. Compared to other fiber-optic sensors, our sensor features an extremely simple structure and fabrication process, and hence cost effectiveness.

Keywords: Optical Fiber Sensor, Multimode Interference, MMI, Curvature Sensor, Temperature Sensor.

1. INTRODUCTION

The measurement of relative displacements and deformations as well as temperature is of great importance in many fields such as aerospace, geophysics, and nanotechnology, in medicine for diagnosis, and in structural health monitoring. Although the deflection of loaded structures is a basic parameter in the field of strength of materials, in practice this quantity is quite difficult to measure [1]. Due to its relation with structural mechanical parameters such as strain, torsion, and position, curvature measuring is of great interest. In spite of the great importance of curvature measuring, there are only a few sensors that can actually measure it [2]. Temperature effects can also play a role for bending structures and it completes the picture of the mechanical conditions under which the element of analysis is operating. Therefore, being capable of measuring both curvature and temperature simultaneously is highly desired. Recently, due to the frequent occurrence of this requirement, there has been a great effort to develop sensors that can measure simultaneously several parameters such as pressure, strain, force, temperature, curvature, and refractive index. It was found that grating-based fiber sensors are suitable for simultaneous-measuring tasks because of their sensitivity to several external parameters. Particularly, Fiber Bragg Grating (FBG) based optical sensors have been extensively investigated and simultaneous-measuring sensors for force-temperature [3], pressure-temperature [4], transversal load-temperature [5], and refractive index-temperature [6] have been reported. FBG sensors for strain-temperature simultaneous measuring have been even more widely investigated and several techniques have been developed in this area [7-8].

Although some FBG-based sensors for simultaneous measuring of curvature and temperature have been reported [9-11] they still present some disadvantages. In general, FBG-based sensors are associated with complex and expensive manufacturing procedures since they need special equipment to print the grating on the fiber; tilted-FBG- and SFBG-based (i.e. super-structure fiber Bragg grating) sensors clearly need a more complex fabrication process since the grating planes are sloped by an angle in relation to the longitudinal fiber axis and both FBG and LPFG are printed on the fiber,

respectively. One problem commonly associated with LPG sensors is the low accuracy for measuring their resonant peak shifts due to their large resonant bandwidths [12]. Since a FBG is sensitive to both temperature and strain, it is difficult to determine whether the wavelength shift is introduced by temperature or strain when the FBG sensor is used in a variable temperature environment. In spite of the numerous investigations that have been carried out to address this problem the complete discrimination between thermal and bending effects has not been fully achieved.

On the other hand, sensors based on multimode fiber (MMF) have been previously investigated but there is a particular effect that occurs in MMF that has not been explored for measurements of curvature and temperature. The multimode interference (MMI) effect occurs in MMF and is related to the formation of periodic images of the field coupled into the MMF that can be found at well defined locations. Devices based on MMI effects such as MMI optical coupler devices [13], MMI splitters for sensing applications [14], and MMI switches [15] have been reported. Since MMI devices exhibit a pass-band filter response the wavelength response can be used for sensing applications. Sensing devices based on MMI effects have been used as displacement sensors [16], band-pass filters [17], as well as their use to provide single-transverse-mode laser emission from multimode active fibers [18]. In this work we propose a novel fiber device based on MMI effects for independent measurement of curvature and temperature with self-discrimination of thermal and bending effects. Such device can be potentially used for simultaneous measurement of curvature and temperature since their response to each parameter is uncorrelated.

2. MULTIMODE INTERFERENCE SENSOR

The fabrication of the MMI sensor is quite simple. The only components required are a MMF, which is spliced between two single-mode fibers (SMF), as shown in Fig. 1.



Figure 1. Schematic of the MMI sensor.

The operation of the MMI filter is as follows. The key component is a MMF that supports several modes (≥ 3). After the supported modes are excited by launching a field using the input SMF, the interference between the modes propagating along the MMF gives rise to the formation of self-images of the input field along the MMF. Therefore, the length of the MMF has to be precisely cleaved in order to have a self-image right at the face of the output SMF. The MMI effect has been previously studied and the length of the MMF can be calculated using

$$L = p \left(\frac{3L_\pi}{4} \right), \quad p = 0, 1, 2, 3, \dots \quad (1)$$

In the previous equation L_π is the beat length, which is defined as follows:

$$L_\pi = \frac{4\eta_{MMF} D_{MMF}^2}{3\lambda_0} \quad (2)$$

Where η_{MMF} and D_{MMF} are the refractive index and diameter of the MMF core, respectively, and λ_0 is the free-space wavelength. As shown in Eq. (1), self-images should be periodically formed along the MMF. However, due to the nature of the MMI effect, the true images of the input field are given at every fourth image. The images formed at other locations are known as pseudo-images, and although they resemble the input field they exhibit higher losses. Therefore, we operate our MMI sensors at the fourth image.

If the length of the MMF is properly calculated, the transmitted intensity against wavelength exhibits a band-pass response. The experimental result of a MMI sensor is shown in Fig. 2. The filter response is due to the fact that images

are formed wherever the phase accumulated by the modes is a multiple of 2π , and this occurs at the peak wavelength of the filter. As we deviate from this wavelength, the images are formed before or after the MMF-SMF interface, resulting in a reduced signal coupled to the SMF output.

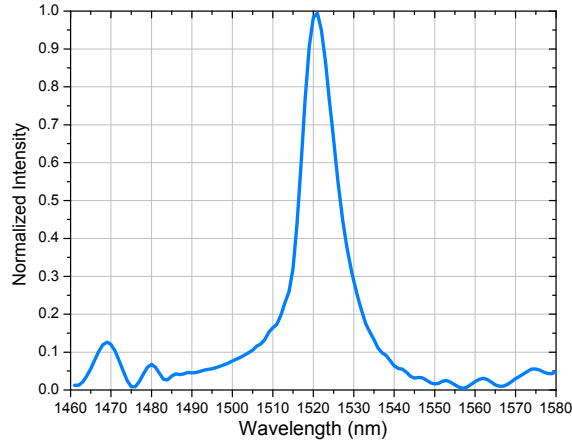


Figure 2. Experimental wavelength response of the MMI fiber filter using No-Core fiber.

In order to use the MMI as a sensor, we take advantage that the propagation angle of the modes in the MMF can be modified by bending the fiber. As the fiber is bended the amplitude of the modes is reduced, and since the image is the result of the interference of such modes, thus the image will exhibit lower peak intensity. As shown in Eq. (2), the peak wavelength is determined by both the wavelength and the structural characteristics of the fiber and the peak wavelength remains the same during bending. When the fiber is heated, structural as well as refractive index changes will occur that can modify the peak wavelength response of the MMI sensor. Therefore, temperature can be monitored by following changes in the peak wavelength response of the MMI device.

3. EXPERIMENTAL SETUP AND RESULTS

In our experiments we used a special fiber known as No-Core fiber, which is basically a $125\ \mu\text{m}$ MMF with air as its cladding. The advantage of this fiber is that it provides a narrower band-pass response, due to the higher refractive index contrast between core and cladding (air). The MMI sensor was characterized using a tunable laser (wavelength range from 1460 to 1580 nm) and a photodetector connected to a digital multimeter. The whole setup was fully controlled using LabVIEW. In the case of temperature measurements, a standard ring laser cavity was built to further narrow the MMI response and being able to detect the peak wavelength shifts.

3.1 Curvature Sensing

Bending of No-Core MMF was tested by using two translation stages (i.e. one fixed and one movable), with the sensor attached to both stages, as shown in Fig. 3. The fiber was carefully aligned to avoid twisting during bending and it was fixed so that the section of MMF remained in the middle of the setup while bending the fiber.

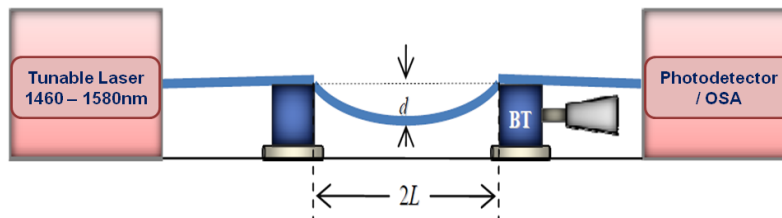


Figure 3. Experimental setup for curvature measurement.

In the previous configuration the curvature (or the radius of curvature) can be calculated using,

$$\rho = \frac{1}{R} = \frac{2d}{(d^2 + L^2)} \quad (3)$$

where d is the vertical displacement of the fiber with respect to the horizontal line defined when the fiber is not bent, and L is half of the separation distance. The distance between the translation stages was 300 mm. The No-Core MMF was evaluated in the range of curvature from 0 to 1.059883m^{-1} , which corresponds to a vertical displacement from 0 to 12 mm. The response of the No-Core sensor in the wavelength range from 1460-1580 nm for the previous curvature range is shown in Fig. 4(left). The inset in Fig. 4 (left) shows a zoom of the peaks; as explained before, it can be clearly seen that the peak wavelength only varies on its intensity.

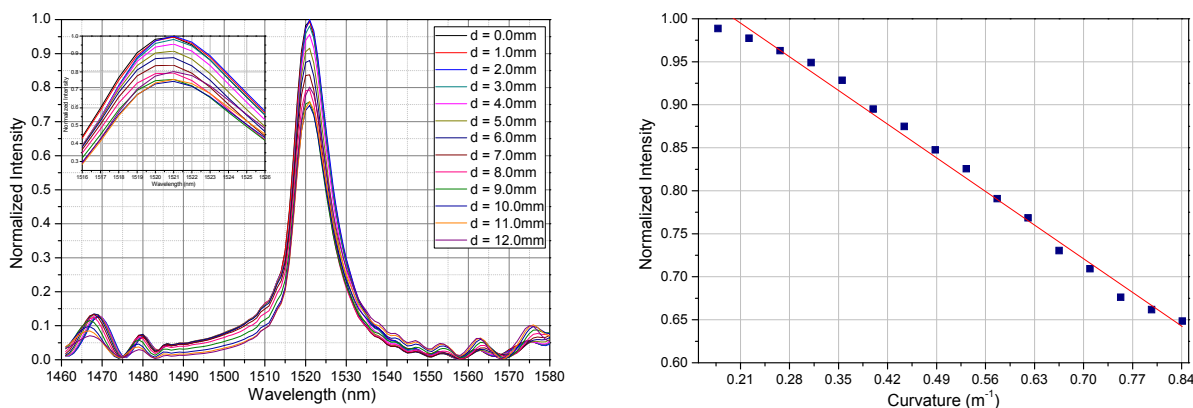


Figure 4. Experimental results of curvature measurements (left), and Intensity versus inverse radius of curvature (right).

The filter response clearly shows a similar waveform for all cases and the peak wavelength remains at the same value. On the other hand when the curvature increases the intensity of the peak decreases. By plotting the peak intensity versus inverse radius of curvature we can notice that we obtain a linear response within some range of curvature, as shown in Fig. 4(right). Nevertheless, the sensor exhibit very low sensitivity for small curvatures (i.e. less than 0.17m^{-1}). This can be corrected by inducing a pre-bending to the fiber so it can detect the smallest changes.

3.2 Temperature Sensing

When a fiber is heated we can expect some modification to the fiber dimensions (diameter and length) due to the thermal expansion coefficient, as well as refractive index changes as a result of the thermo-optic effect. All these effects can be taken into account by using the following equation, which is based on Equations (1) and (2),

$$\Delta\lambda = p \left[\frac{(\eta + \Delta\eta)(D + \Delta D)^2}{L + \Delta L} \right] - \lambda_0 \quad (4)$$

where $\Delta L = L\alpha\Delta T$ and $\Delta D = D\alpha\Delta T$ are the increment in length and diameter respectively, with $\Delta n = \sigma\Delta T$ as the refractive index change. The thermal expansion coefficient ($\alpha = 0.5 \times 10^{-6}/^\circ\text{C}$) and thermo optic coefficient ($\sigma = 7 \times 10^{-6}/^\circ\text{C}$) are used for a silica fiber [19]. As will be later shown, the dominant term is the thermo-optic effect.

Since the thermo-optic effect is very small, we do not expect a huge peak wavelength shift. According to Eq. (4) a shift of no more than 5 nm is expected with a temperature of 400°C . Therefore, an MMI sensor with a peak wavelength of 1550.08 nm was placed inside a standard ring cavity laser with Erbium doped fiber as the gain media. The MMI sensor

acts as a filter, and lasing is achieved at the peak wavelength. This effectively narrows the bandwidth, and allows for detection of small temperature changes. The output of the ring laser is monitored using an Optical Spectrum Analyzer (OSA). In order to uniformly increase the temperature around the MMI sensor an aluminum channel surrounding the fiber was used. The temperature is controlled with a hot plate and a maximum stable temperature of 375°C was obtained. The temperature is monitored with a thermocouple and the MMI sensor, as well as the thermocouple, are not in contact with the aluminum channel. Measurements were made in a temperature range from 25°C to 375°C and the spectrum was taken at every 25 °C temperature interval. As shown in Fig. 5 (left), there is a wavelength shift of approximately 4.5 nm when the temperature reaches 375°C. We should also notice that the wavelength is increased, which corroborates that the dominating term is the thermo-optic effect. By plotting the peak wavelength as a function of temperature, we can also notice that we have a nice linear response, as shown in Fig. 5 (right). We also show the response as calculated from Eq. (4), see red line.

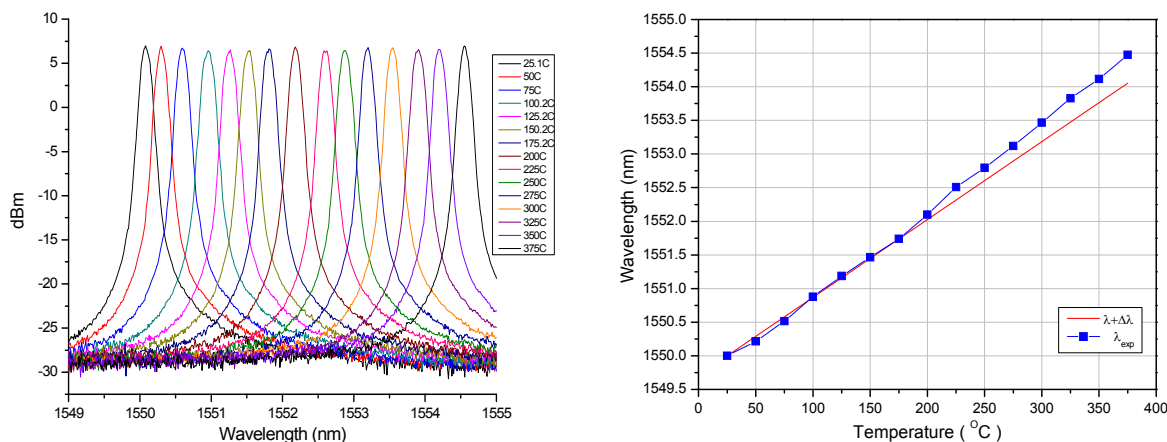


Figure 5. Sensor response for different temperatures in the operation range from 25-375°C.

We should highlight that the peak intensity does not exhibit a significant change as the temperature is increased. This is important since curvature is measured by following intensity changes in the peak wavelength. This provides a simple way to measure both curvature and temperature not only at the same time but both measurements are decoupled from each other.

4. CONCLUSION

A novel self-discrimination fiber optic sensor based on MMI effects for independent measurement of curvature and temperature has been proposed, implemented, and tested. The operating mechanism of the proposed sensor is based on monitoring of the peak wavelength shift and its intensity when the temperature and curvature are modified, respectively. Curvature and temperature measurements have been independently performed due to the fact that the amplitude of the peak wavelength varies with the curvature while the peak wavelength remains at the same value; and, on the other hand, the peak wavelength shifts when temperature varies while the intensity remains invariant. Furthermore, operating ranges where the sensor exhibits linear responses were defined for both curvature and temperature measurements. Compared to other fiber-optic curvature and temperature sensors, our sensor features an extremely simple structure and fabrication process, and hence a very low cost and reproducible sensor. Since we can have a different peak wavelength by just changing the MMF length, multiplexing and several-point remote sensing are straightforward. By using an appropriate material, high temperature sensor should be also feasible.

REFERENCES

- [1] Kovacevic M, Nikezic D, Djordjevich A. "Monte carlo simulation of curvature gauges by ray tracing". *Meas. Sci. Technol.* **15**(1756), 61 (2004).
- [2] Yili Fu, HaitingDi. "Fiber-optic curvature sensor with optimized sensitive zone". *Optics and Laser Technology* **43**, 586–591 (2011).
- [3] Weigang Zhang, Xiaoyi Dong, Qida Zhao, Guiyun Kai, and Shuzhong Yuan. "FBG-Type Sensor for Simultaneous Measurement of Force (or Displacement) and Temperature Based on Bilateral Cantilever Beam". *IEEE Photonics Technology Letters*, 13(12), 1340-1342 (2001).
- [4] Guanghui Chen, Liying Liu, Hongzhi Jia, Jimin Yu, Lei Xu, Wencheng Wang. "Simultaneous pressure and temperature measurement using Hi-Bi fiber Bragg gratings". *Optics Communications* **228**, 99–105 (2003).
- [5] Rao Yun-Jiang, Wang Yi-Ping, Zhu Tao, and Ran Zeng-Ling. "Simultaneous Measurement of Transverse Load and Temperature using a Single Long-Period Fiber Grating Element". *Chinese Physics Letters* **20**(1), 72-75 (2003).
- [6] Tao Zhu, Yun-Jiang Rao, and Qiu-Ju Mo. "Simultaneous Measurement of Refractive Index and Temperature Using a Single Ultralong-Period Fiber Grating". *IEEE Photonics Technology Letters*, 17(12), 2700-7002 (2005).
- [7] Guanghui Chen, Liying Liu, Hongzhi Jia, Jimin Yu, Lei Xu, and Wencheng Wang. "Simultaneous Strain and Temperature Measurements With Fiber Bragg Grating Written in Novel Hi-Bi Optical Fiber. *IEEE Photonics Technology Letters*, 16(1), 221-223 (2004).
- [8] Young-Geun Han, Suho Song, Gil Hwan Kim, Kwanil Lee, Sang Bae Lee, Ju Han Lee, Chang Hyun Jeong, Chi Hwan Oh, and Hee Jeon Kang. "Simultaneous independent measurement of strain and temperature based on long-period fiber gratings inscribed in holey fibers depending on air-hole size". *Optics Letters* **32**(15), 2245-2247 (2007).
- [9] B.A.L. Gwandu, X. Shu, Y. Liu, W. Zhang, L. Zhang, and I. Bennion. "Simultaneous and independent sensing of arbitrary temperature and bending using sampled fibre Bragg grating". *Electronics Letters*, 37(15), 946-948 (2001).
- [10] R. Falate, O. Frazão, G. Rego, O. Ivanov, H. J. Kalinowski, J. L. Fabris, J. L. Santos. "Bend and Temperature Sensing with Arc-Induced Phase-Shifted Long-Period Fiber Grating". *Optical Society of America (OSA), Proceedings of the Annual Meeting of the, TuE43* (2006).
- [11] Qiang Wu, Agus Muhamad Hatta, Pengfei Wang, Yuliya Semenova, Gerald Farrell. "Use of a Bent Single SMS Fiber Structure for Simultaneous Measurement of Displacement and Temperature Sensing". *Dublin Institute of Technology, Articles of the School of Electronic and Communications Engineering*, 1(1), (2010).
- [12] Du, Weichong; Tam, Hwayaw; Liu, Michael S.; Tao, X. M., "Long-period fiber grating bending sensors in laminated composite structures". *Proc. SPIE, Vol. 3330*, pp. 284-292 (1998).
- [13] L. B. Soldano, F. B. Veerman, M. K. Smit, B. H. Verbeek, A. H. Dubost, and E. C. M. Pennings, "Planar monomode optical couplers based on multimode interference effects," *J. Lightwave Technol.* **10**(12), 1843–1850 (1992).
- [14] D. A. May-Arrijoja, P. LiKamWa, J. J. Sanchez-Mondragon, R. Selvas-Aguilar, and I. Torres-Gomez, "A reconfigurable multimode interference splitter for sensing applications," *Meas. Sci. Technol.* **18**(10), 3241–3246 (2007).
- [15] D. A. May-Arrijoja, N. Bickel, and P. LiKamWa, "Robust 2x2 multimode interference optical switch," *Opt. Quantum Electron.* **38**(7), 557–566 (2006).
- [16] A. Mehta, W. Mohammed, and E. G. Johnson, "Multimode interference-based fiber-optic displacement sensor," *IEEE Photon. Technol. Lett.* **15**(8), 1129–1131 (2003).
- [17] W. S. Mohammed, P. W. E. Smith, and X. Gu, "All-fiber multimode interference bandpass filter," *Opt. Lett.* **31**(17), 2547–2549 (2006).
- [18] X. Zhu, A. Schülzgen, H. Li, L. Li, Q. Wang, S. Suzuki, V. L. Temyanko, J. V. Moloney, and N. Peyghambarian, "Single-transverse-mode output from a fiber laser based on multimode interference," *Opt. Lett.* **33**(9), 908–910 (2008).
- [19] G. B. Hocker, "Fiber-optic sensing of pressure and temperature", *Applied Optics*, Vol. 18, Issue 9, pp. 1445-1448 (1979).